Ecol Res (2015) 30: 311–325
DOI 10.1007/s11284-015-1254-6

SPECIAL FEATURE

Long-term and interdisciplinary research on forest ecosystem functions: Challenges at Takayama site since 1993

Ayaka Wenhong Kishimoto-Mo · Seiichiro Yonemura
Masaki Uchida · Miyuki Kondo · Shohei Murayama
Hiroshi Koizumi

Contribution of soil moisture to seasonal and annual variations of soil CO_2 efflux in a humid cool-temperate oak-birch forest in central Japan

Received: 30 September 2014 / Accepted: 18 February 2015 / Published online: 5 March 2015

Abstract To quantify the contribution of soil moisture to seasonal and annual variations in soil CO_2 efflux in a cool-humid deciduous broadleaf forest, we measured soil CO_2 efflux during the snow-free seasons of 2005–2008 using an automated chamber technique. This worked much better than manual chambers employing the same steady-state through-flow method. Soil CO_2 efflux (g C m^{-2} $period^{-1}$) during the snow-free season ranged from 979.8 ± 49.0 in 2005 to 1131.2 ± 56.6 in 2008 with a coefficient variation of 6.4 % among the 4 years. We established two-parameter (soil temperature and moisture) empirical models, finding that while soil temperature and moisture explained 69–86 % and 10–13 % of the temporal variability, respectively. Soil moisture had the effect of modifying the temporal variability of soil CO_2 efflux, particularly during summer and early fall after episodic rainfall events; greater soil moisture enhanced soil CO_2 efflux in the surface soil layers. High soil moisture conditions did not suppress soil CO_2 efflux, leading to a positive correlation between normalized soil CO_2 efflux (ratio of the measured to predicted efflux using a temperature-dependent Q_{10} function) and soil moisture. Therefore, enhanced daily soil CO_2 efflux following heavy rainfall events could significantly reduce net ecosystem exchange (i.e. daily net ecosystem production) by 32 % on some days. Our results highlight the importance of precisely estimating the response of soil CO_2 efflux to changes in soil moisture following rainfall events when modeling seasonal carbon dynamics in response to climate change, even in humid monsoon regions.

Keywords Automated soil respiration chambers · Empirical model · Open-flow IRGA method · Rainfall · Soil respiration

Electronic supplementary material The online version of this article (doi:10.1007/s11284-015-1254-6) contains supplementary material, which is available to authorized users.

A. W. Kishimoto-Mo (✉) · S. Yonemura
National Institute for Agro-Environmental Sciences (NIAES),
3-1-3 Kannondai, Tsukuba, Ibaraki 305-8604, Japan
E-mail: mow@affrc.go.jp
Tel.: 029-838-8194 (0)
Fax: 029-838-8199

M. Uchida
National Institute of Polar Research (NIPR), Tachikawa,
Tokyo 190-8518, Japan

M. Uchida
SOKENDAI (The Graduate University for Advanced Studies),
Tachikawa, Tokyo 190-8518, Japan

M. Kondo
National Institute for Environmental Studies (NIES),
Tsukuba 305-8506, Japan

S. Murayama
National Institute of Advanced Industrial Science and Technology
(AIST), Tsukuba 305-8569, Japan

H. Koizumi
Laboratory for Environmental Ecology, Waseda University,
Tokyo 169-8555, Japan

Introduction

Forests in the middle and high latitudes of the northern hemisphere create a significant sink for atmospheric carbon (C; Fang et al. 2014). Natural broadleaf deciduous forests in Japan contribute to this large global C sink (Saigusa et al. 2002, 2005; Fang et al. 2014). A forest C sink, measured as net ecosystem production (NEP), balances two opposing biological processes, photosynthetic assimilation (net primary production, e.g. tree growth) and heterotrophic respiration (Ohtsuka et al. 2009). That is, NEP represents the balance between gross primary production and ecosystem respiration of forests (Saigusa et al. 2002). Soil CO_2 efflux (R_s) or soil respiration, including autotrophic respiration from roots and heterotrophic respiration from microbes and soil fauna, is therefore an important process that regulates the C balance in forest ecosystems. In fact, R_s typically contributes 30–80 % of annual total ecosystem respiration in forests (Davidson et al. 2006b), and even >90 % in some years (Mo et al. 2005a). Identifying the sources and quantifying the magnitudes of variation in R_s are critical to assessing the influence of forests ecosystems on atmospheric CO_2 concentrations in a world experiencing climate change.

Soil temperature and moisture are two important abiotic parameters affecting R_s and related underlying processes in terrestrial ecosystems (e.g. Davidson et al. 1998; Lee et al. 2002, 2008; Mo et al. 2005b; Hashimoto et al. 2009; Kim et al. 2010; Wang et al. 2010), although primary productivity and litter fall supply are also critical drivers (Davidson et al. 2002; Kuzyakov and Gavrichkova 2010). For instance, at the global scale, R_s increased linearly with mean annual temperature but responded non-linearly to mean annual precipitation in naturally-regenerated forests (Wang et al. 2010). On a seasonal time scale, a strong exponential increase in R_s with soil temperature has been found across a wide range of terrestrial ecosystems (see a review in Davidson and Janssens 2006). This led to widespread use of the Q_{10} function in studies of the temporal variation in soil CO_2 efflux (Oishi et al. 2013). The Q_{10} function (see Eq. 5 in "Materials and Methods") is comprised of two parameters where Q_{10} is the sensitivity of R_s to temperature and R_{10} is the basal rate of respiration at the reference temperature of 10 °C. Measures of Q_{10} and R_{10} derived from field data may integrate confounding effects from the sensitivity of both variables to temperature as well as their sensitivity to seasonal changes in physiological activities induced by photosynthesis, root phenology, microbial biomass, and other factors (Mo et al. 2005b; Davidson et al. 2006a). This so-called "apparent Q_{10}" should be interpreted cautiously and quantified by specifying both spatial and temporal scales (Davidson and Janssens 2006; Kirschbaum 2010). Despite this, the Q_{10} function can still provide a useful empirical tool for estimating annual R_s and comparing R_s among sites (Curiel Yuste et al. 2005; Mo et al. 2005b). The increasing use of automated chamber systems for measuring soil CO_2 efflux makes Q_{10} function particularly valuable (Lee et al. 2008; Kim et al. 2010; Oishi et al. 2013).

Soil moisture is considered the second most important environmental parameter affecting R_s; low soil moisture directly limits microbial activity, while high soil moisture reduces air-filled soil porosity and may limit the diffusion of soil gases especially in agricultural soils (Davidson et al. 1998; Lee et al. 2002; Yonemura et al. 2009). Soil rewetting following a rainfall event is a critical factor regulating soil CO_2 efflux and other soil gas fluxes (see Kim et al. 2012 for a recent review). Curiel Yuste et al. (2005) estimated that ~9 to 14 % of annual R_s in an oak forest in Belgium was rainfall induced, with soil temperature the main factor controlling annual R_s. Globally precipitation patterns have been predicted to change with increasing intra-annual variability and more frequent extremes (IPCC 2013). Thus, knowledge of the relative contribution of soil moisture to both seasonal and annual R_s is particularly important in regions where profound changes in precipitation are expected. Japan, one such region, has forests covering complex terrain with a typical oceanic climate and abundant precipitation that are strongly affected by monsoons (Saigusa et al. 2005). Using a model, Hashimoto et al. (2011) estimated that total R_s in Japan's forests would be equivalent to ~39 % of the total C emissions from fossil-fuel combustion and other anthropogenic activities in Japan (350 Tg C year^{-1}, in 2008). Lee et al. (2006) reviewed soil respiration of forest ecosystems in Japan (N = 51) and demonstrated that, although soil temperature was usually the dominant control on R_s, changes in soil moisture following rainfall events and typhoons cause abrupt changes in R_s. Therefore, estimating and predicting the contribution of soil moisture to R_s in Japan's forests is important because it relates directly to Japan's commitment to the Kyoto Protocol and future C sequestration strategies.

This study quantified the contribution of soil moisture to seasonal and annual variations in soil CO_2 efflux in a humid cool-temperate deciduous broadleaf forest in central Japan. The Takayama flux site (hereafter, TKY), the oldest forest site of the AsiaFlux network, has experience more than two decades of long-term monitoring yielding many important findings related to C pools and flows in this ecosystem (e.g. Lee et al. 2002, 2006; Saigusa et al. 2002, 2005; Jia et al. 2003; Mo et al. 2005a, b; Satomura et al. 2006; Ohtsuka et al. 2007, 2009). Ohtsuka et al. (2007) and Ohtsuka et al. (2009) have reported on detailed of C cycling of this forest. Previous studies on R_s (1999–2002) found that soil temperature was the primary factor affecting variations in R_s at this site (Mo et al. 2005b), while rainfall-induced soil CO_2 release accounted for 16–21 % of the annual R_s (Lee et al. 2002). Furthermore, prolonged soil drying after the rainy season in summer created low levels of daily soil CO_2 efflux (Mo et al. 2005b). However, these findings were developed from low frequency measurements (biweekly to monthly) using manual soil respiration chambers, which limited the documentation of the short-term effects on soil CO_2 efflux immediately following rainfall events. We wanted to improve on the quantity and quality of data collected using an automated chamber technique based on the previously used open-flow infrared gas analyzer (IRGA) method (Lee et al. 2002; Mo et al. 2005a, b). We used this technique to measure soil CO_2 efflux during the snow-free seasons from 2005 to 2008. Fortunately, Yonemura et al. (2013) installed CO_2 sensors to continuously measure the vertical CO_2 concentration in the soil profile at this study site from June 2005 through May 2006, thereby establishing a diffusion model that can be used to estimate vertical CO_2 emission from each 1-cm layer at soil depths of 0–50 cm. Our objectives were to examine the performance of the automated chamber technique relative to the diffusion model, and to quantify R_s in response to changes in soil moisture using high-frequency data collections. We wanted to explore the possible mechanisms controlling vertical soil CO_2 emissions (Yonemura et al. 2013) and the seasonal patterns of NEP and root respiration (Lee et al. 2005). Additional objectives were to estimate annual R_s with and without considering soil moisture using an empirical model approach, and to discuss the contribution of soil moisture to annual R_s at this forest site.

Materials and methods

Site description

TKY, located in central Japan (36°08′N, 137°25′E, 1420 m a.s.l), experiences a cool temperate climate under the influence of the Asian monsoon. Mean annual temperature and precipitation (1994–2009) were 6.5 °C, measured at 25-m height using a flux tower, and 2056 mm at the Takayama Forest Research Station, Institute for Basin Ecosystem Studies, Gifu University, which is ~0.5 km south of TKY site (http://www.green.gifu-u.ac.jp/takayama/Data.html), respectively. This secondary broad-leaved deciduous forest grew on a brown forest soil (*Dystric Cambisols*), specifically, well-drained acidic sandy loams mixed with volcanic ash (Yonemura et al. 2013 provides detailed soil information). A permanent 1 ha (100 × 100 m^2) plot on a west-facing slope had allowed the study biometric based estimates of NEP (Ohtsuka et al. 2007, 2009). Dominant broad-leaved deciduous species included *Quercus crispula* (27 % of basal area), *Betula ermanii* (25 %) and *Betula platyphylla* var. *japonica* (15 %), with a few evergreen conifer species (3 %; Ohtsuka et al. 2009). Japanese beech (*Fagus crenata*) dominated the primary climax vegetation around the permanent plot. However, the planting of coppice oak (*Quercus crispula*) forests for the production of charcoal had largely replaced these climax forests, although these charcoal-production forests were abandoned when the demand for charcoal declined rapidly after the 1960s. Thus, 15–20 m tall coppice oak mixed with deciduous pioneer trees, all approximately 50–60 years old, uniformly covered the plot. A very dense *Sasa senanensis* community (a perennial evergreen dwarf bamboo; 100 % coverage; ~40 stems m^{-2}; 1–1.5 m tall) covered the forest floor. Budding and leaf shedding occurred in May and October, respectively, and snow usually covered the ground from December to April.

The first forest flux-tower site of AsiaFlux network, established here in 1993 using a 27-m tall tower using an aerodynamic method, provided continuous measurements of the net CO_2 flux [net ecosystem CO_2 exchange (NEE) ≈ NEP] between the forest and atmosphere; the eddy covariance method replaced this in 1998 (e.g. Saigusa et al. 2002, 2005). Eddy covariance-based NEE was estimated at 2.59 Mg C ha^{-1} $year^{-1}$ (1999–2006), comparable to the biometric-based NEP estimate (2.1 ± 1.15 Mg C ha^{-1} $year^{-1}$), suggesting the forest is a steady sink of atmospheric CO_2 (Ohtsuka et al. 2007, 2009). Saigusa et al. (2005) provided detailed measurement descriptions of NEE with eddy covariance. The AsiaFlux database (http://www.asiaflux.net/) provided the CO_2 flux data (NEE) for TKY.

Measurement of the soil CO_2 efflux using automated vs. manual chambers

Diurnal changes in CO_2 efflux from soil and snow surfaces at TKY have been measured continuously for 24–48 h once or twice a month by the open-flow IRGA method with manual open/close chambers from 1995 to 2002 (Mo et al. 2005a, b). The open-flow method, or so-called steady-state through-flow method, is very reliable for determining soil CO_2 efflux (Pumpanen et al. 2004). In 2005, we established the automatic opening and closing chamber (AOCC) technique instead of using the manual chamber technique based on the same open-flow IRGA method, to observe soil CO_2 efflux continuously throughout the year except for snow seasons. We used four automated chambers (five starting in 2007), each with a 20-cm internal diameter, 25 cm tall, and set 5 cm into the soil. Chambers were deployed in the same area reported by Mo et al. (2005a, b), around the flux tower where NEE was observed using the eddy covariance method (e.g. Saigusa et al. 2002; 2005).

Suh et al. (2006) and Lee et al. (2008) used a similar concept for their AOCC system. The AOCC system employed three main parts: an automated chamber unit (SENSA Corporation, Inagi, Tokyo, Japan) that opened/closed with air pressure driven by a compressor, a pumping and relay control unit (Japan ANS Co. Ltd., Fuchu, Tokyo, Japan), and a computer that ran the relay program and logged data (software by Japan ANS Co. Ltd.). The pumping system employed a buffer tank made from a commercial 30 L plastic box, three air pumps (JN022ANE and N86KNE, KNF Neuberger GmbH, Freiburg, Germany), three electric cooling units (Japan ANS Co. Ltd.), and five mass-flow controllers (SEC-B40, HORIBA STEC Co., Ltd., Kyoto, Japan). When measuring soil CO_2 efflux, air from the buffer tank pumped into the IRGA CO_2 analyzer and inlet of the chamber at a flow rate of 1.35 L min^{-1}, as well as controlled the flow of air from the outlet at the same rate using another pump. The CO_2 concentration of the chamber inlet and outlet air were measured with a dual-channel CO_2 analyzer (BINOS 100 2 M, Emerson Process Management, Manufacturing GmbH & Co., OHG, Hasselroth, Germany) with a flow rate of 0.2 L min^{-1} after removal of water vapor by an electric cooling unit, while the remaining sample air was vented. Soil CO_2 efflux rate was calculated as the difference in CO_2 concentration between the inlet and outlet of the chamber when operating in a steady state condition (e.g. Bekku et al. 1997; Lee et al. 2002; Pumpanen et al. 2004; Mo et al. 2005b; Suh et al. 2006; see Eq. 1 for the calculations). In our study, the CO_2 concentration inside of the chamber reached a steady-state with a flow rate of 1.35 L min^{-1} at 25–35 min after chamber closure, varying with seasons (data not shown). Therefore, the CO_2 concentration at 39–40 min after chamber closure was used to calculate the efflux rate (see Eq. 1). Accordingly, 40, 160 and 200 min were required for one, four, and five chamber measurements to complete one measurement cycle, respectively. Mean hourly efflux was calculated from each measuring cycle in ~3-h intervals (e.g. Fig. 1b, d). The CO_2 analyzer was automatically calibrated with standard CO_2 gases at four concentrations (pure N_2 gas as a zero CO_2 base and air-based CO_2 standard gases of 350, 700, 995 ppm) after the fourth cycle. The computer saved environmental data (e.g. atmospheric pressure, cell temperature of the CO_2 analyzer, soil temperature inside the chambers) and CO_2 concentration, allowing remote access to the data from our research institute.

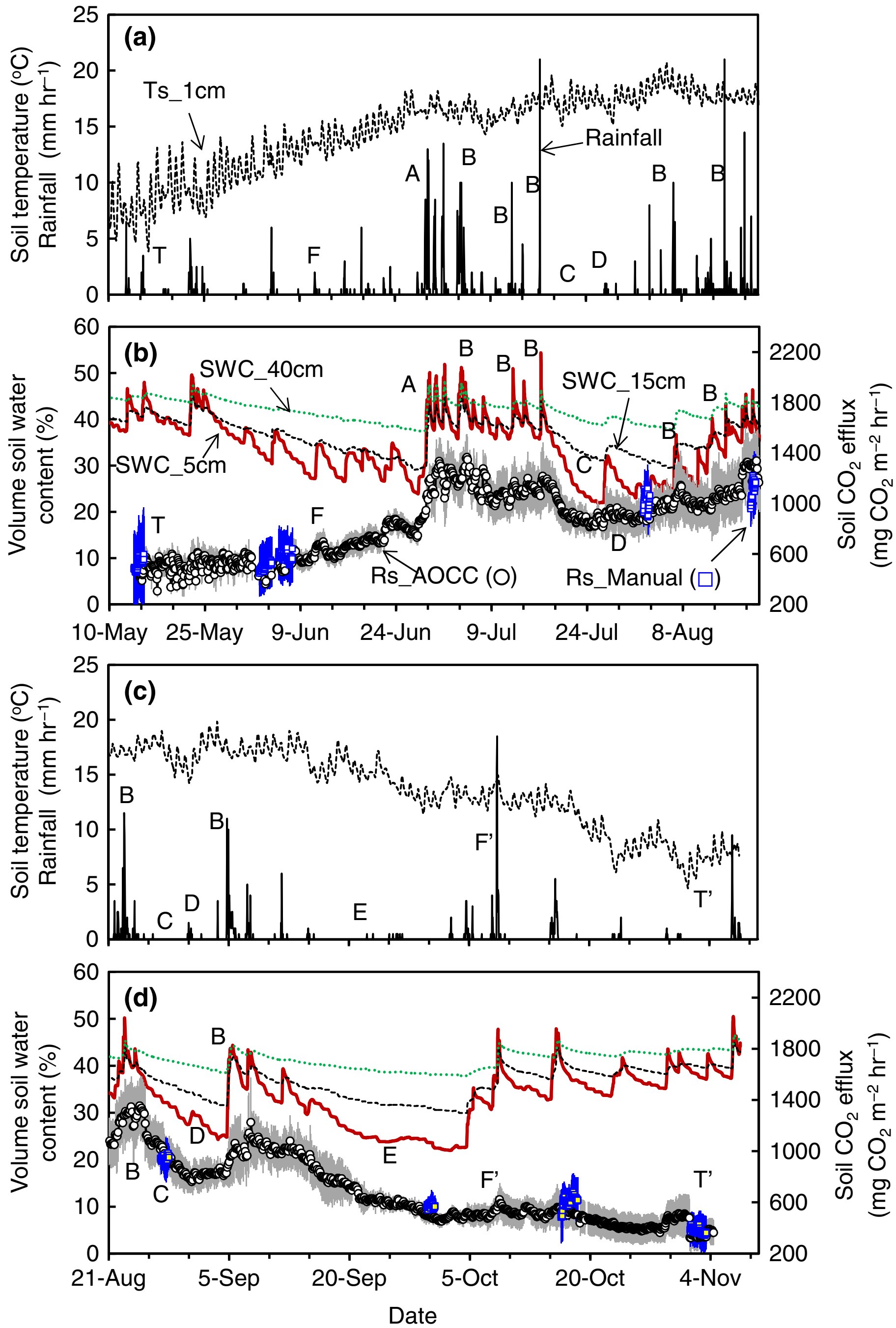

Fig. 1 Seasonal changes in soil temperature and rainfall (**a**, **c**), soil moisture and hourly CO_2 efflux by automated and manual chamber techniques (**b**, **d**) from May 10 to August 20 (**a**, **b**) and from August 21 to November 10 (**c**, **d**), 2005. *Error bars* represent the standard deviation of four chambers. The points labelled A, B, C, D, E, F, F′, T and T′ indicate changes in the efflux with the timing of rainfall (see the "Results" section for details)

In 2005, soil CO_2 efflux was also measured with four manual chambers using the same open-flow system of Mo et al. (2005a, b) to allow comparison with data collected using the AOCC technique. Each manual chamber was placed 0.8–1.0 m from an AOCC chamber. Manual chambers were made of PVC material, with a 21 cm internal diameter, 15 cm tall, and set 5 cm into the soil. A 2.5 cm high PVC lid was placed on top of each chamber immediately before measurements were started. A measurement cycle of 25 min for the four chambers was repeated. Soil CO_2 efflux was measured continuously for 24 h to obtain daily efflux. Natural surface litter was retained within either manual or automated chambers; however, live and/or standing dead vegetation was carefully removed prior to the experiment. Mo et al. (2005b) provides additional information related to the measuring system used with manual chambers.

Environmental variables

Environmental data related to air temperature, soil temperature and moisture (as volumetric soil water content) were collected from a location adjacent to chambers, as described previously (Saigusa et al. 2002; Mo et al. 2005b; Yonemura et al. 2013). Soil temperature was monitored at a single location by thermocouples at depths of 1, 10, 20, and 50 cm, except that three thermocouples were used at three points 1 cm deep. Soil moisture was measured at a single location by time domain reflectometry (TDR, Model CS612, Campbell Scientific, Logan, UT, USA) at depths of 5, 10 and 20 cm, except that two points were used at 5 cm deep. Snow depth was measured near the tower ultrasonically (SR50 acoustic sensor; Campbell Scientific). Data for all parameters were averaged hourly and daily.

Data analyses

Using the open-flow method, the soil CO_2 efflux rate (mg CO_2 m^{-2} h^{-1}) was calculated as the difference in CO_2 concentration between inlet and outlet of the chamber at a steady state condition (Eq. 1):

$$R_{s\_hourly}\left(\text{mg } CO_2 m^{-2} h^{-1}\right) = \left(\Delta CO_2 \times 10^{-6} \times L \times 10^{-3} \times \rho \times 10^{6}\right) \times 60 \times A^{-1} \tag{1}$$

where ΔCO_2 is the difference in the CO_2 concentrations between the inlet and outlet of the chamber at a steady state condition (ppm), L is the flow rate (L min^{-1}), and ρ is the density of CO_2 (kg m^{-3}). A is the soil surface area (m^2) covered by the chamber. The constants in the equation convert the units to mg CO_2 m^{-2} h^{-1} (Suh et al. 2006).

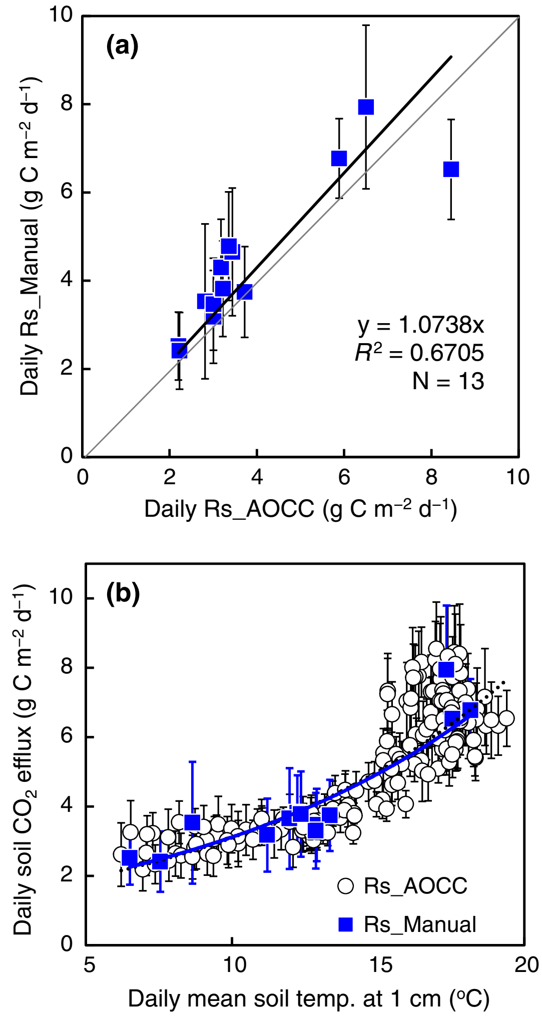

Fig. 2 Comparison of soil CO_2 efflux measured by the two chamber techniques (AOCC vs. Manual) in the snow-free seasons of 2005. **a** Mean daily efflux and **b** the relationship between daily efflux to soil temperature at 1 cm depth. *Error bars* represent the standard deviation of four chambers from each technique

For each chamber the daily total soil CO_2 efflux (daily R_s, g C m^{-2} day^{-1}) was calculated as the mean of the hourly efflux estimates (e.g. 3-h intervals for AOCC) of the day, multiplying 24 h and converting the unit to g C m^{-2} day^{-1}. Thus, mean daily R_s was the mean of daily R_s from four to five AOCC chambers or four manual chambers (e.g. Figs. 2b, 3c, 4a). We reported daily efflux instead of hourly efflux to prevent confounding results associated with diurnal fluctuations, which usually peaked around 5 pm during the snow-free season (Yonemura et al. 2013). Daily R_s was plotted against daily mean soil temperature at 1 cm using an exponential model (e.g. Figs. 2b, 4a) to determine the relationship between soil temperature and soil CO_2 efflux:

$$Fc_{(Ts)} = a \times e^{bTs} \tag{2}$$

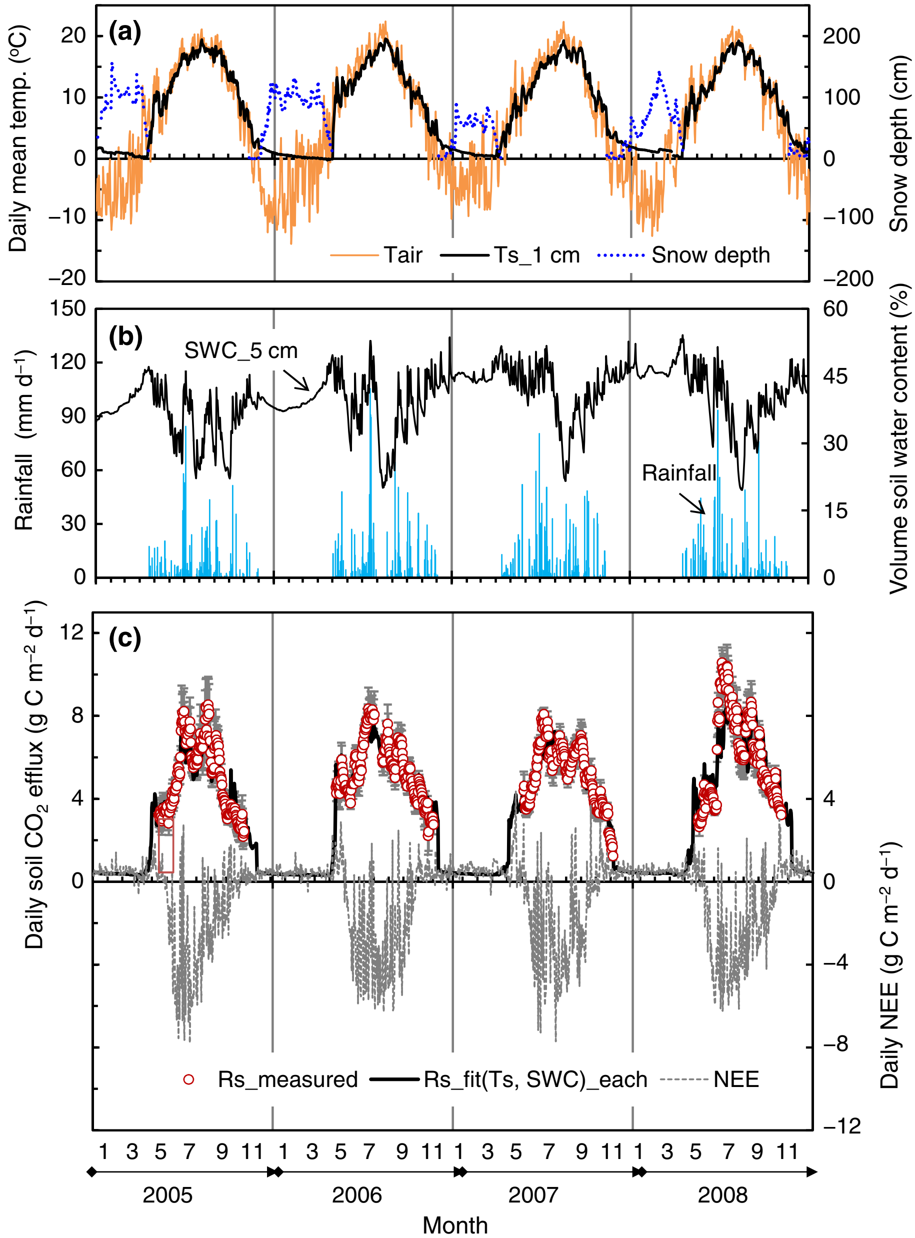

Fig. 3 Seasonal variation in **a** daily mean air (at 27 m), soil temperature at 1 cm and snow depth; **b** daily rainfall and volume soil water content; and **c** mean daily soil CO_2 efflux (R_s) and net ecosystem CO_2 exchange based on tower eddy covariance in 2005–2008. *Error bars* represent the standard deviation of four (2005–2006) or five (2007–2008) AOCC chambers. Estimated R_s ($R_{s\_fit\_each}$) was calculated using Fit (11) to Fit (15) for the snow-free seasons in 2005 to 2008, respectively, and Fit (16) for estimating the winter CO_2 efflux from the date of initial snow-cover and 15 days after snow melt; see Table 1 for the parameters for Fit (11) to Fit (16)

The reference respiration rate at 10 °C (R_{10}, same unit as $Fc_{(Ts)}$), was calculated as:

$$R_{10} = a \times \ e^{10b} \qquad (3)$$

By definition, the value of Q_{10} (sensitivity to temperature) was calculated from the differences in the respiration rate at a temperature interval of 10 °C. Using the exponential model (Eq. 2), Q_{10} was considered conceptually constant with temperature:

$$Q_{10} = Fc_{(Ts+10)}/Fc_{(Ts)} = e^{10b} \qquad (4)$$

Combining Eq. (3) and (4), Eq. (1) can be expressed as a Q_{10} function:

$$Fc_{(Ts)} = R_{10} \times Q_{10}^{((Ts-10)/10)} \qquad (5)$$

where soil CO_2 efflux [$Fc_{(Ts)}$] was the predicted CO_2 efflux (g C m^{-2} day^{-1}) at soil temperature Ts (°C) at a depth of 1 cm.

To examine soil CO_2 efflux in response to the soil water content (volumetric SWC, %), normalized efflux [$Fc'_{(SWC)}$] was calculated as:

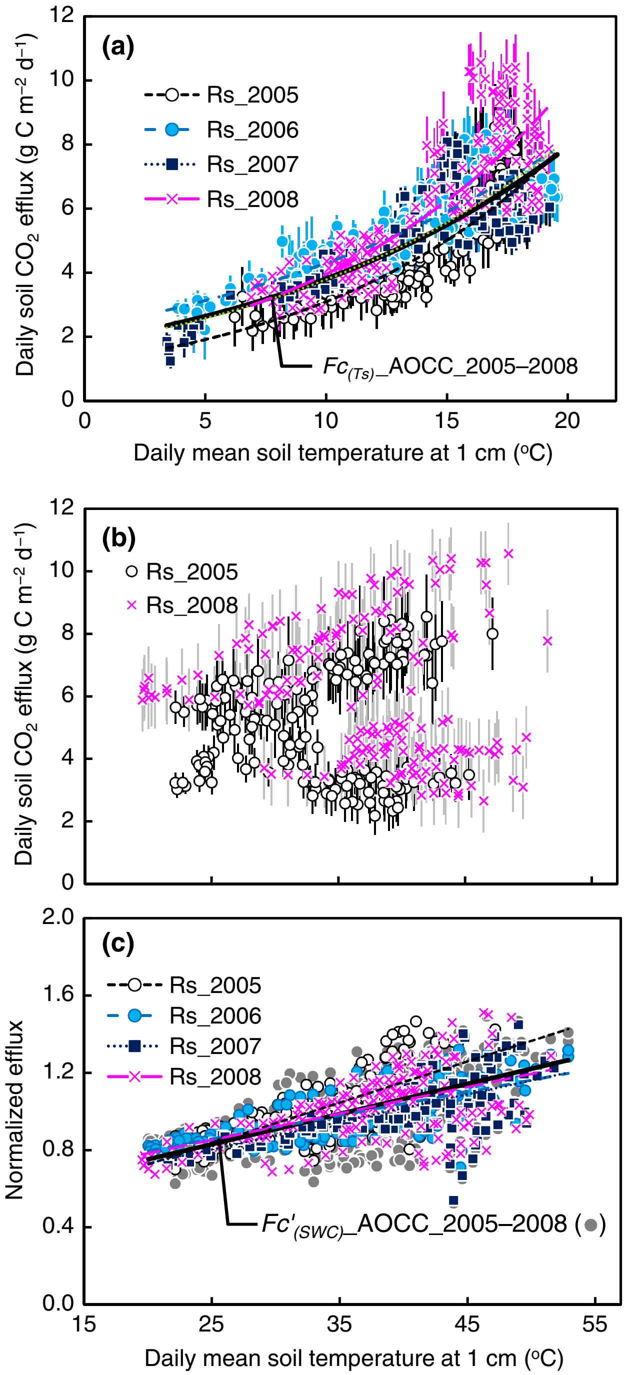

Fig. 4 Relationship between soil CO_2 efflux and **a** soil temperature and **b** soil water content in the snow-free seasons. Soil CO_2 efflux after normalization of the effect of soil temperature is plotted against soil moisture in (**c**); the legend symbols are the same as (**a**). *Error bars* in **a** and **b** represent the standard deviation of four (2005–2006) or five (2007–2008) AOCC chambers. Normalized efflux ($Fc'_{(SWC)}$) = measured efflux/predicted efflux by soil temperature (Eq. 5, $Fc_{(Ts)}$ in (**a**), respectively). See Table 1 for the parameters for all fitted functions

$$Fc'_{(SWC)} = \text{Measured efflux at}_{Ts} / \text{Predicted efflux by Eq. 5 } [Fc_{(Ts)}] \quad (6)$$

and plotted against daily mean SWC using linear regression (e.g. Fig. 4b):

$$Fc'_{(SWC)} = A \times SWC + B \quad (7)$$

where soil CO_2 efflux [$Fc'_{(SWC)}$] was the predicted CO_2 efflux (g C m^{-2} day^{-1}) at *SWC* (%) at a depth of 5 cm after normalizing the effect of soil temperature and *A* and *B* were parameters fitted for 2005–2008 data (Fig. 4b; Table 1).

By combining Eqs. (5) and (7), we established a simple empirical model to estimate daily soil CO_2 efflux (g C m^{-2} day^{-1}) using soil temperature and soil moisture during snow-free seasons:

$$Fc_{(Ts,SWC)} = Fc_{(Ts)} \times Fc'_{(SWC)} \quad (8)$$

Results

Comparison of manual and automated chamber techniques (manual vs. AOCC)

Data for seasonal changes in soil CO_2 efflux measured with AOCC from early spring to middle summer (Fig. 1b) and from middle summer to late autumn (Fig. 1d) were in agreement with data from manual chambers. The daily pattern of hourly R_s measured by the two techniques also showed similar trends (Fig. S1). Daily soil CO_2 efflux from the mean of four AOCC chambers was not significantly different from data of manual chambers (Fig. 2a; N = 13, $P > 0.05$). The AOCC technique had the advantage of providing continuously measured CO_2 efflux throughout the seasons (Fig. 1b, d). The relationship between daily soil CO_2 efflux and soil temperature showed no significant difference, irrespective of chamber technique (Fig. 2b, see Table 1 for fitted functions). However, the AOCC technique improved to the capture of the effects of soil temperature, rainfall, and soil moisture events on soil CO_2 efflux (Fig. 1). Hourly R_s (3-h intervals) increased with soil temperature after snow melt, showing sensitivity to soil temperature at 1 cm from day to day (Fig. 1b, point T). A small increase in R_s with rainfall was also observed (Fig. 1b, point F). R_s measured with AOCC increased with soil temperature from 400 to 600 mg CO_2 m^{-2} h^{-1} from late spring to late June. AOCC captured a rapid response of R_s (600 to 1400 mg CO_2 m^{-2} h^{-1}) to soil moisture, which increased dramatically (25–50 %) following heavy rainfall at the end

Table 1 The fitted coefficients in used Figs. 2b and 4 and the fitted functions for the estimation of soil CO_2 efflux with and without considering the effects of soil moisture

	Code[a]	$Fc_{(Ts)} = R_{10} \times Q_{10}^{((Ts-10)/10)}$		$Fc_{(SWC)} = A \times SWC + B$		R^2	N	Source
		R_{10}	Q_{10}	A	B			
Fit (1a)	$Fc_{(Ts)}$_Manual_1995	1.857	2.61	–	–	0.8402	21	Mo et al. (2005a)
	$Fc_{(Ts)}$_Manual_1999–2002	2.471	2.58	–	–	0.8172	52	Mo et al. (2005b)
	$Fc_{(Ts)}$_Manual_2005	3.119	2.52	–	–	0.8510	13	
Fit (1b)	$Fc_{(Ts)}$_AOCC_2005	3.100	2.62	–	–	0.7631	173	This study, Fig. 2b, 4a
Fit (2)	$Fc_{(Ts)}$_AOCC_2006	4.300	1.89	–	–	0.7654	184	This study, Fig. 4a
Fit (3)	$Fc_{(Ts)}$_AOCC_2007	3.780	2.17	–	–	0.7998	176	This study, Fig. 4a
Fit (4)	$Fc_{(Ts)}$_AOCC_2008	3.957	2.50	–	–	0.7634	169	This study, Fig. 4a
Fit (5)	$Fc_{(Ts)}$_AOCC_2005–2008	3.811	2.08	–	–	0.7072	702	This study, Fig. 4a
Fit (6)	$Fc'_{(SWC)}$_AOCC_2005	–	–	0.0213	0.3006	0.5488	173	This study, Fig. 4c
Fit (7)	$Fc'_{(SWC)}$_AOCC_2006	–	–	0.0122	0.5518	0.4862	184	This study, Fig. 4c
Fit (8)	$Fc'_{(SWC)}$_AOCC_2007	–	–	0.0413	0.4460	0.4071	152	This study, Fig. 4c
Fit (9)	$Fc'_{(SWC)}$_AOCC_2008	–	–	0.0137	0.5095	0.2959	169	This study, Fig. 4c
Fit (10)	$Fc'_{(SWC)}$_AOCC_2005–2008	–	–	0.0156	0.4388	0.4160	702	This study, Fig. 4c
Fitted functions for the estimations of snow-free seasons and annual soil respiration using two parameters (soil temperature and moisture)								
Fit (11)	$Fc_{(Ts,SWC)}$_AOCC_2005 $= Fc_{(Ts)} \times Fc'_{(SWC)} =$ Fit (1b) $\times$ Fit (6)							
Fit (12)	$Fc_{(Ts,SWC)}$_AOCC_2005 $= Fc_{(Ts)} \times Fc'_{(SWC)} =$ Fit (2) $\times$ Fit (7)							
Fit (13)	$Fc_{(Ts,SWC)}$_AOCC_2005 $= Fc_{(Ts)} \times Fc'_{(SWC)} =$ Fit (3) $\times$ Fit (8)							
Fit (14)	$Fc_{(Ts,SWC)}$_AOCC_2005 $= Fc_{(Ts)} \times Fc'_{(SWC)} =$ Fit (4) $\times$ Fit (9)							
Fit (15)	$Fc_{(Ts,SWC)}$_AOCC_2005 – 2008 $= Fc_{(Ts)} \times Fc'_{(SWC)} =$ Fit (5) $\times$ Fit (10)							
Fit (16)[b]	$Fc_{(Ts)}$–Snowsurfaceefflux	2.036	6.38	–	–	0.8782	14	Mo et al. (2005b)

[a] All fitted functions were significant ($P < 0.001$)

[b] See Table 1, Fit (5) in Mo et al. (2005b) Agr For Meteorl 134:81–94, using for the estimation of winter CO_2 efflux (including efflux from the snow surface during the period of snow cover and from the soil surface until 15 days after snowmelt)

of June (Fig. 1b, point A). During the warm season from July to August when soil temperature remained at 15–22 °C, AOCC also captured pulses of R_s following rainfall events (Fig. 1b, d, points B). At the end of July and during August (point C in Fig. 1), R_s decreased gradually as soil moisture decreased; that is, decreases in R_S reflected soil drying after the rainy season (Fig. 1b, point C) and typhoons (Fig. 1d, point C), even though the soil temperature remained high. R_s declined from 1000 to 400 mg CO_2 m^{-2} h^{-1} from early September to autumn when soil temperature and moisture declined (Fig. 1d, point E). R_s was less responsive to an increase in soil moisture after October when soil temperature was < 15 °C (Fig. 1d, point F′). A sudden decrease in R_s (from 470 to 340 mg CO_2 m^{-2} h^{-1}) occurred when soil temperature dropped to < 5 °C (Fig. 1d, point T′).

The effects of soil temperature and moisture on the seasonal variation in soil CO_2 efflux

Mean annual air temperature at a height of 25-m was 6.0, 6.7, 6.7, and 6.6 °C from 2005 to 2008, respectively (Fig. 3a; Table 2). A snowpack that formed in early December every year kept soil temperatures above 0 °C at 1 cm deep (Fig. 3a), as also reported by Mo et al. (2005b). The length of the snow-free season in 2005 to 2008 was 224 days (Apr 20 to Nov 29), 215 days (May 1 to Dec 2), 216 days (Apr 10 to Nov 11), and 215 days (Apr 18 to Nov 18), respectively (Fig. 3a).

Soil moisture was generally high during winter, but usually peaked in spring when snow melted, and varied with rainfall amounts during the snow-free season (Figs. 1b, 3b). June and July is the rainy season at the study site and typically experiences large amounts of rainfall. The Japan Meteorological Agency (http://www.data.jma.go.jp/fcd/yoho/baiu/kako_baiu08.html) documented the length of the rainy season in the area surrounding TKY as follows: 38 days (Jun 11 to Jul 18, 2005), 49 days (Jun 8 to Jul 26, 2006), 44 days (Jun 14 to Jul 27, 2007), and 46 days (May 28 to Jun 12, 2008). Total rainfall in those periods was 401, 600, 476, and 419 mm, respectively (Fig. 3b). Soil moisture was generally high in the rainy season and low after the rainy season. Several typhoons in late August and September resulted in increased soil moisture.

Over the course of the snow-free season, soil CO_2 efflux generally fluctuated in parallel with seasonal changes in soil temperature (Fig. 3a, c). That is, soil temperature exerted principle control on the seasonal variability of soil CO_2 efflux (Fig. 4a; see Table 1 for fitted functions). Accordingly, the Q_{10} function [Fit (1b) to Fit 4 in Table 1] inferred that soil temperature explained 69 to 86 % of the variability in daily soil CO_2 efflux during the snow-free season during the four study years (86.4, 83.1, 83.5 and 68.7 % for 2005–2008 respectively, according to the correlation coefficients of Q_{10} functions with measured R_s, $P < 0.001$).

Variations in soil moisture caused the temporal variability of soil CO_2 efflux especially during summer and early fall (Figs. 1b, d, 3c). A plot of daily soil CO_2 efflux against soil moisture for 2005 and 2008 (Fig. 4b) indicated a confounding effect with soil temperature, as temperature and moisture were significantly correlated (e.g. in snow-free season of 2005, $r = -0.554$, $P < 0.001$, N = 224). However, normalized soil CO_2 efflux, the ratio of the measured efflux to the predicted efflux using the temperature-dependent Q_{10} function (Eq. 4), was significant and positively correlated with soil moisture in the snow-free season (Fig. 4c; see Table 1 for each fitted function). This demonstrated that the increase of soil moisture following rainfall events enhanced daily soil CO_2 efflux. These high moisture events sometimes switched daily NEE from being a C sink (negative values) to C source (positive values) in the rainy and typhoon seasons (Fig. 3c, Fig. S2). Therefore, enhanced soil CO_2 efflux following rainfall events may contribute to these NEE pulses (Fig. 3c), although the low gross primary production occurring with low solar radiation caused by cloud cover may be the major controlling factor (Saigusa et al. 2005). For instance, a crude estimate (Fig. S2) showed that enhanced daily soil CO_2 efflux following heavy rainfall events during 27 June to 4 July, 2005 (ΔR_s, 12.8 g C m^{-2}) may contribute to reducing the NEE (Δ NEE, 40.3 g C m^{-2}) by 32 % on these days.

The two-parameter (*Ts* and *SWC*) models (i.e. Fit 11 to Fit 14 in Table 1) explained 80–96 % of the variability in daily soil CO_2 efflux (96.4, 96.0, 93.9 and 79.5 % for 2005–2008 respectively, based on the correlation coefficients of model estimates of measured R_s, $P < 0.001$). Separately, soil temperature explained 69–86 % of the temporal variability in daily soil CO_2 efflux, while soil moisture explained an additional 10–13 % (10, 13, 10 and 11 % for 2005–2008, respectively).

Annual soil respiration (R_s) from 2005–2008

Table 2 summarizes several estimates of annual R_s using the fitted functions in Table 1. Because measured soil CO_2 efflux with AOCC covered 78–88 % of the snow-free season, the sum of measured efflux could provide a standard for evaluating estimated R_s using different fitted functions (empirical models). Annual R_s estimated by Q_{10} function, the single parameter related to soil temperature, derived from each target year (i.e. Fit 1b to Fit 4) had < 2 % deviation from the cumulative CO_2 efflux ($R_{s\_measured}$). The estimated annual R_s calculated using the two parameters of soil temperature and moisture had < 1.2 % deviation from $R_{s\_measured}$. However, if empirical models derived from the average of the 4 years were used (i.e. Fits 5 and 10), deviation from $R_{s\_measured}$ increased to > 10 % regardless of whether soil moisture was considered or not. This sug-

Table 2 Estimation of snow-free season and annual soil respiration (R_s) by different regression equations of Table 1

Year	Air temp. at 25 m[a] (°C)	Precipitation[a] (mm $year^{-1}$)	Snow-free seasons	Annual soil respiration		Deviation to measured annual R_s (%)			
			R_s_measured[b] (g C m^{-2} $period^{-1}$)	R_s_measured[b] (g C m^{-2} $year^{-1}$)	R_s_estimated[c] (g C m^{-2} $year^{-1}$)	$Fc^{d}_{(Ts,\,SWC)}$		$Fc^{d}_{(Ts)}$	
						Each year	All	Each year	All
2005	6.0	1953	979.8 (49.0)	1045.9 (52.3)	1034.1 (51.7)	−1.13	+4.11	−2.60	+7.51
2006	6.7	2187	1112.8 (55.6)	1180.5 (59.0)	1169.9 (58.5)	−0.90	−7.49	−0.40	−7.71
2007	6.7	1956	1057.0 (52.9)	1124.6 (56.2)	1115.5 (55.8)	−0.81	+2.46	−1.59	−2.41
2008	6.6	1819	1131.2 (56.6)	1213.4 (60.7)	1219.5 (61.0)	+0.51	−9.62	−0.20	−10.46
Mean[e]	–	–	1070.2 (68.1)	1141.1 (73.3)	1134.8 (79.4)	–	–	–	–
Corrected R_s^f	–	–	909.7 (57.9)	969.9 (55.0)	964.6 (67.5)	–	–	–	–

[a] Annual mean air temperature from eddy-tower at the study site [Takayama (TKY) flux site, near Takayama city, Japan]. Precipitation data from the Takayama Research Station, Institute for Basin Ecosystem Studies, Gifu University (~500 m south of the TKY site)

[b] Sum of measured soil CO_2 efflux by automatic opening and closing chamber and by gap-filling by R_s_estimated[c] if there was any missing data. Values in parenthesis represent the standard error (N = 4 for 2005–2006 and N = 5 for 2007–2008)

[c] See Table 1 and Fits (11) to (15) for the estimation of snow-free seasons for each year, 2005–2008, respectively, and Fit (16) for the winter soil CO_2 efflux. Values in parenthesis represent the standard error (N = 4 for 2005–2006 and N = 5 for 2007–2008)

[d] See Table 1, for "Each year" Fit (1b) to Fit (4) for each target year, and Fit (5) for all (fitted with mean measured efflux of 2005–2008)

[e] Mean for 2005–2008. Values in parenthesis represent the standard error of the 4 years, and same in Corrected R_s^f

[f] Topographic correction (annual $R_s \times 0.85$) was used to estimate annual soil respiration for the 1-ha plot at the TKY site (see Mo et al. 2005b)

gested that the relationship of soil CO_2 efflux to soil temperature and/or soil moisture was specific to each year. The value of Q_{10} ranged from 1.89 to 2.62 for each year (i.e. Fit 1b to Fit 4), and was 2.08 when all 4 years of data were combined (Fit 5). The Q_{10} value was lowest (1.89) in 2006, while R_{10} was highest. Although the Q_{10} function derived from each target year could be used to estimate annual R_s with a similar accuracy using the two parameters of soil temperature and moisture (Table 2), the Q_{10} functions overestimated soil CO_2 efflux during the post-rainy season in August during dry down of the soil (Fig. 5b). The two-parameter empirical models (i.e. Fit 11 to Fit 14) predicted daily soil CO_2 efflux fairly well with AOCC-measured efflux (Fig. 5b). However, the empirical models all underestimated daily soil CO_2 efflux when the measured efflux was >8 g C m^{-2} day^{-1}, irrespective of whether soil moisture was considered or not (data not shown). Therefore, the empirical models underestimated soil CO_2 efflux in the rainy season (e.g. part of June and July), although the two-parameter model derived from each target year always provided the best fit (Fig. 5b).

Soil CO_2 efflux (g C m^{-2} $period^{-1}$) during the snow-free season ranged from 979.8 ± 49.0 in 2005 to 1131.2 ± 56.6 in 2008 with coefficient variation of 6.4 % among the 4 years (Table 2). The large efflux of CO_2, occurring in July 2008, contributed greatly to the highest annual R_s (Fig. 5a; Table 2). We topographically corrected annual R_s of the 1-ha experimental plot (Table 2) following Mo et al. (2005b) to allow comparison with previous studies (Mo et al. 2005b; Ohtsuka et al. 2007, 2009).

Discussion

Contribution of soil moisture to soil CO_2 efflux coupled with soil temperature and other factors

Soil temperature, the major environmental driver of soil CO_2 efflux at our site (Fig. 4a), explained 69–86 % of the variability in R_s in the four investigated years. This agrees with previous studies (Mo et al. 2005a, b) and many other studies of soil CO_2 efflux in temperate and cool-temperate forests in the Asian monsoon area (Lee et al. 2008; Hashimoto et al. 2009; Kim et al. 2010; Joo et al. 2012). Generally in these forests, soil moisture also modulates soil CO_2 efflux following soil rewetting after periods of dryness. In a previous study at our site (Lee et al. 2002), daily soil CO_2 efflux increased substantially after rainfall in summer (rainy-day efflux was 1.6 times that of a typical sunny day) when measuring efflux every 2 weeks with manual chambers. High-frequency measurements with AOCC in this study confirmed a previous finding by Lee et al. (2002) that soil CO_2 efflux increased with increasing soil moisture in the rainy season and following rain events in the typhoon season (Figs. 1, 3).

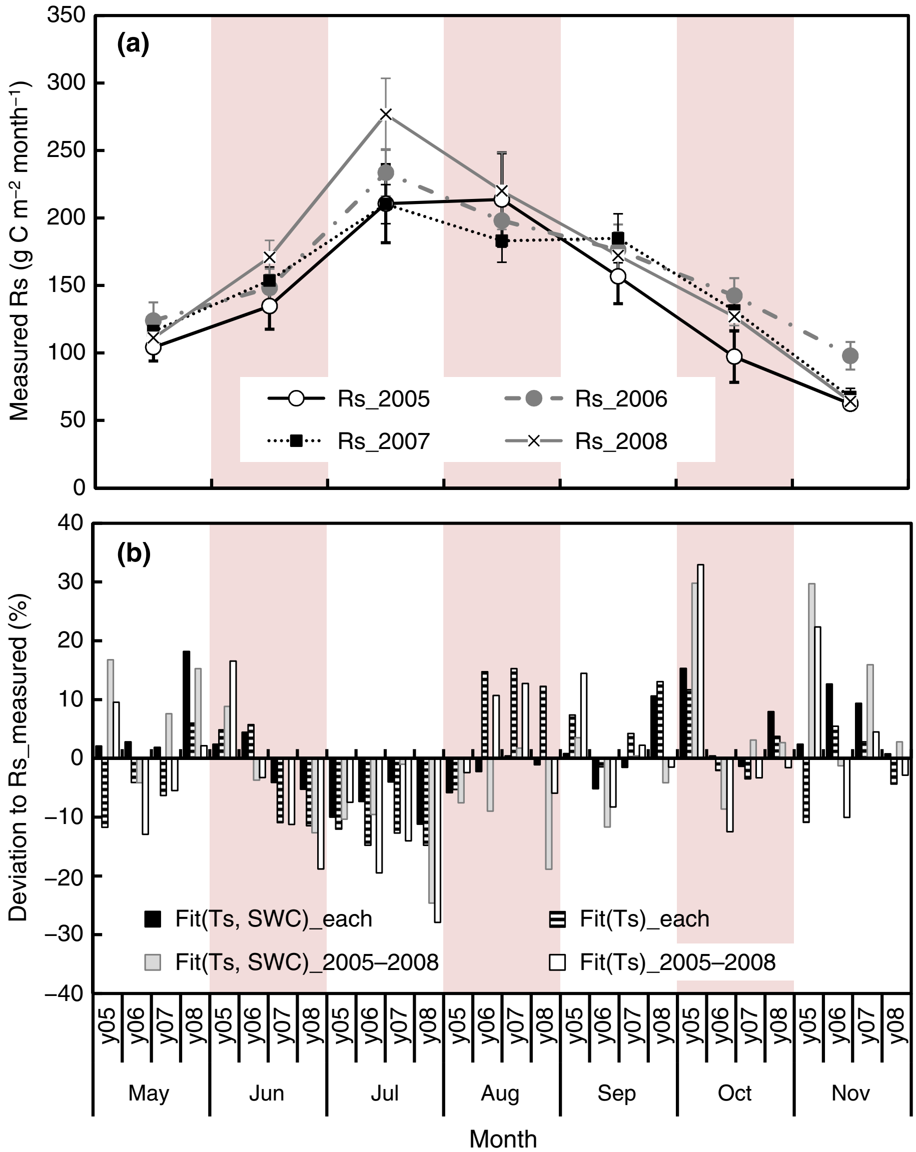

Fig. 5 Comparison monthly soil CO_2 efflux in 2005–2008 measured with the AOCC technique and estimated using empirical models. **a** Monthly soil CO_2 efflux measured with the AOCC technique in 2005–2008. *Error bars* represent the standard deviation of four (2005–2006) or five (2007–2008) AOCC chambers; **b** the deviation of predicted monthly soil CO_2 efflux using different fitted functions to the measured efflux. See Table 1 for the parameters for all fitted functions

We also compared the daily CO_2 efflux from the soil surface using AOCC to the vertical CO_2 emissions from different soil layers estimated by the diffusion model of Yonemura et al. (2013) (Fig. 6). The diffusion model was based on soil-air CO_2 concentrations adjacent to the AOCC chambers from June to November in 2005, and that experiment was therefore conducted under the same conditions as with AOCC measurements. Decomposition of litter and soil organic matter in shallow soil layers (0–20 cm, including the Oi, Oe and A horizons) was the major contributor to soil CO_2 efflux (Fig. 6b; see Yonemura et al. 2013 for details). Accordingly in warm seasons (late June to early September) the 0–10 cm layer contributed 45–75 % of total R_s, while the contribution of the 10–20 cm layer was moderate and constant (22–26 %) and that of the AB layer (roughly 20–50 cm) was low (about 6–20 %). The surface soil layer, especially the Oi and Oe horizons, could dry out rapidly because the high porosity of the litter layer allowing surface water to evaporate (Yonemura et al. 2013). The process of drying would cause a gradually decline in soil CO_2 efflux (e.g. Fig. 1, points C), while soil rewetting following rainfall could contribute to a burst of CO_2 emission from the C-enriched surface layer (Fig. 1, points B and D). Figure 7b gives examples of soil CO_2 efflux following drying-rewetting cycles and the contribution of each soil layer. Soil CO_2 efflux decreased from July 17 (7.73 ± 1.17 g C m^{-2} day^{-1}) to July 25 (5.65 ± 0.53 g C m^{-2} day^{-1}) when soil moisture at a depth of 5 cm declined from 37 to 22 % (Fig. 6). This

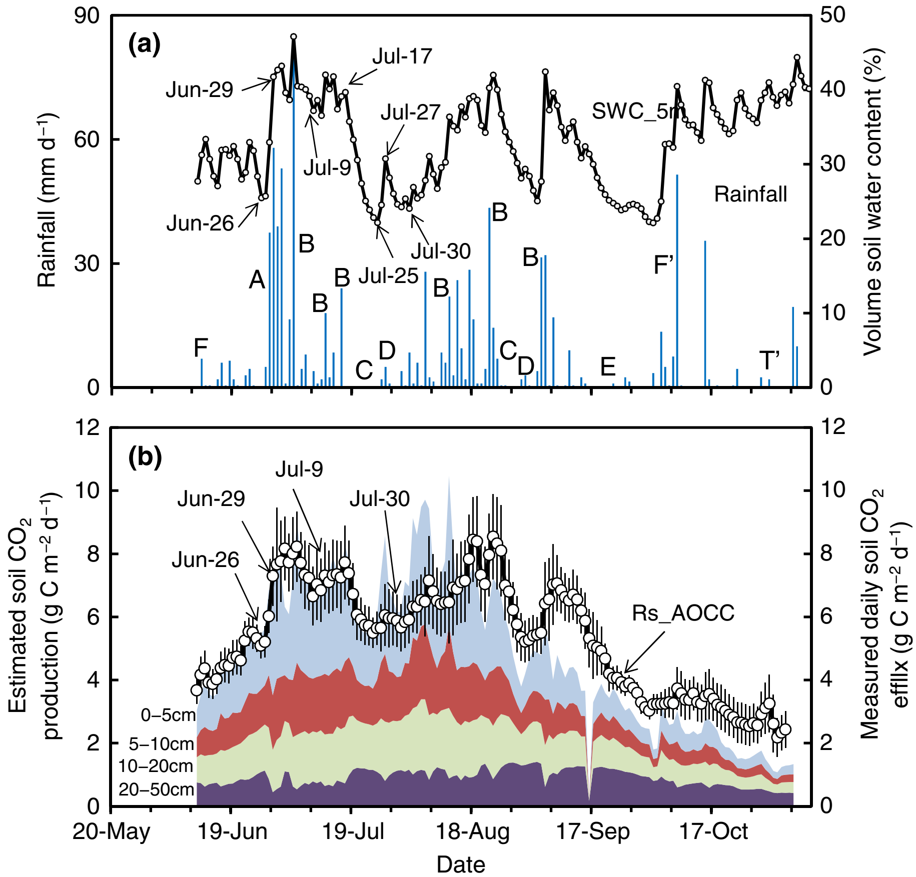

Fig. 6 The contribution of vertical soil CO_2 production (0–5, 5–10, 10–20 and 20–50 cm depth) to the soil surface CO_2 efflux in 2005. **a** Daily rainfall and changes in soil moisture at 5 cm depth. The points labelled A, B, C, D, E, F, F′, and T′ are same as in Fig. 1. **b** Vertical soil emission from different soil layers were estimated by the diffusion model of Yonemura et al. (2013) based on soil CO_2 concentration profiles monitored adjacent to the AOCC chambers. *Error bars* of measured soil CO_2 efflux represent the standard deviation of four (2005–2006) or five (2007–2008) AOCC chambers

decline was consistent with a decline in CO_2 emissions from the 0–5 cm and 5–10 cm layers (Fig. 7b). In contrast, 2 mm of rainfall on July 26 and 5 mm on July 27 caused the soil CO_2 efflux to increase to 6.05 ± 0.98 g C m^{-2} day^{-1} (July 27) because of CO_2 emissions from the 0–10 cm layer. The enhanced soil CO_2 efflux with soil rewetting could be explained by the enhancement of microbial metabolism because of the availability of accumulated substrate during soil drying periods (Kim et al. 2012). The magnitude of the effects of soil rewetting on soil CO_2 efflux may be controlled by size and quality of soil organic matter, properties of soil biota, soil moisture before rewetting, successive moist/wet cycles, soil temperature and an increase in plant photosynthesis following rewetting (Kim et al. 2012). Furthermore, normalized soil CO_2 efflux was positively correlated with soil moisture, suggesting that high-moisture conditions did not cause a reduction in diffusivity and inhibition of CO_2 emissions. Residence time of CO_2 in the soil is ~2 h and even shorter with high moisture (Yonemura et al. 2013). In contrast, Lee et al. (2008) reported a second-order polynomial relationship between normalized soil CO_2 efflux and soil moisture in a Japanese cedar plantation in the same area, i.e. efflux was suppressed during high-moisture conditions. These differences may have been caused by differences in site characteristics, because rice cultivation prior to 1968 at the cedar plantation may have impacted soil porosity and air content. These findings emphasize that gas diffusivity in surface soil should be considered when estimating and predicting the effects of soil moisture on R_s, especially during warm seasons when soil moisture can regulate R_s more than soil temperature (Fig. 1b, d).

The abrupt change in R_s with the dramatic increase in soil moisture at the end of June (Figs. 1, 6; point A) may have been associated with other regulating factors aside from the direct effect of soil rewetting that enhanced microbial metabolism. This peak in R_s coincided with tree leaves expanding rapidly and maturing in late June, coinciding with high photosynthetic capacity (Muraoka and Koizumi 2005). Enhanced photosynthesis could have been a factor that induced an increase in R_s, because photosynthate translocated to roots may have stimulated autotrophic respiration; in addition, root

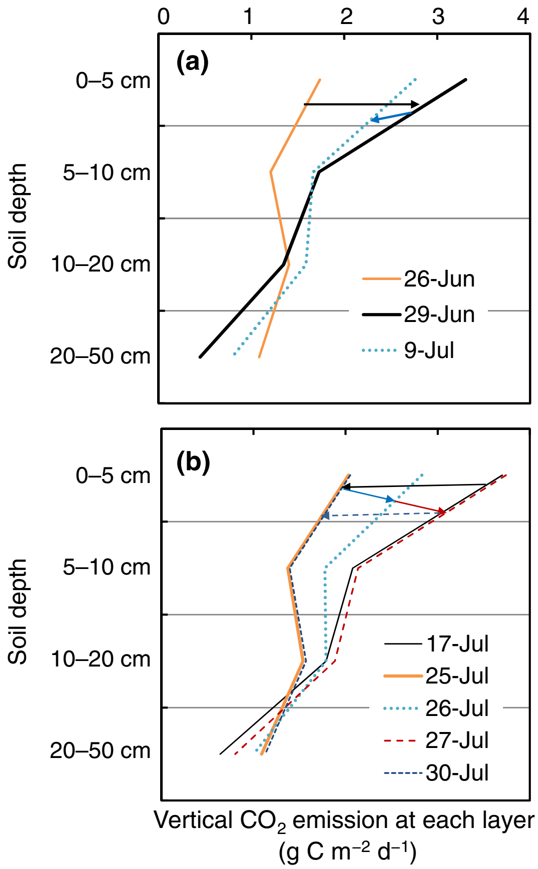

Fig. 7 Vertical profile of daily CO_2 emissions estimated by the diffusion model of Yonemura et al. (2013) before and after rainfall. **a** June 26 (received no rain with soil moisture of 25 %) to June 29 (received 100 mm cumulative rainfall from June 27 to 29 and soil moisture increased to 42 %) and July 9 (mid-rainy season; soil moisture fell to 37 %); **b** July 17 (the end of rainy season with soil moisture at 40 %) following soil drying period to July 25 (soil moisture fell to 22 %), and received 2 mm rainfall in July 26 (soil moisture 25 %) and 5 mm rainfall in July 27 (soil moisture 31 %), followed by drying to July 30 (soil moisture fell to 25 %)

exudates will feed microbes and stimulate microbial respiration (Davidson et al. 2006a; Curiel Yuste et al. 2007). The contribution of root respiration to total R_s was greater in May–June (40–63 %) than in July to September (27–34 %) at our site (Lee et al. 2005). Curiel Yuste et al. (2007) also reported seasonal variations in plant activity (root respiration and exudates production) that exerted a strong influence on seasonal variation of soil metabolic activity in pine plantation and oak savanna ecosystems in California. Obviously, the simultaneously growth of both tree and dwarf bamboo roots could be another explanation for the elevated R_s of point "A" at our site, as has been discussed in Mo et al. (2005b). During autumn when soil temperature was low, R_s was less responsive to changes in soil moisture (Figs. 1d, 6; points E, F′). This could be explained by low soil microbial activity with low soil temperature and a proportionally greater contribution of CO_2 emissions from deeper layers (Fig. 6b) because soil temperature remained warmer in deeper layers (data not shown).

Despite the complexity of the processes that control soil efflux CO_2, empirical models derived from each year had a remarkable predictive ability for R_s during the snow-free season at our study site. The two-parameter (*Ts* and *SWC*) models explained 80–96 % of the variability of the daily soil CO_2 efflux, in which the contribution of soil moisture was 10–13 % of temporal variability. Although the two-parameter models were an improvement over the Q_{10} function, daily soil CO_2 efflux may have still been under- or over-estimated on a seasonal scale (Figs. 5b, 6b). Further development of models will be required if the purpose is to estimate daily soil CO_2 efflux in response to changes in soil moisture. However, regardless of whether soil moisture was included or not, estimated annual R_s had <2 % deviation from measured cumulative CO_2 efflux, if empirical models were derived from each target year. In contrast, if using models derived from the four investigated years (2005–2008), deviation increased to >10 %. Ohtsuka et al. (2009) estimated annual R_s as 791 g C m^{-2} $year^{-1}$ for 2006 using the Q_{10} function derived from 1999–2002 by Mo et al. (2005b), which was 33 % less than the measured annual R_s in this study (Table 2, 1180.5 ± 59.0 g C m^{-2} $year^{-1}$ for 2006). Our results emphasize that empirical models derived from each year could be used for gap-filling purposes, but should be used with caution if applied to other years, since coefficient parameters (e.g. Q_{10}, R_{10}, a, and b in Table 1) may include confounding ecosystem-level responses that are specific to a particular year (Mo et al. 2005a, b; Davidson and Janssens 2006; Kirschbaum 2010; Kuzyakov and Gavrichkova 2010). That is, our results imply that using empirical models derived from the past observations to predict future R_s could cause a 10–30 % over- or under-estimation of annual R_s at our study site.

New findings and challenges for future research

Automated chambers were an improvement over manual chambers using the same open-flow IRGA method. Comparison of the two techniques over the snow-free season of 2005 resulted in no significant difference in soil CO_2 efflux. However, AOCC could provide high-quality data related to soil CO_2 efflux as a function of various abiotic and biotic factors with a high temporal resolution. In this study, we confirmed that the manual chamber technique could provide an adequate estimation of annual R_s if the Q_{10} model was derived from the target year. This observation is helpful in assessing the effects of long-term soil CO_2 efflux on forest C dynamics at our site. Our manual chamber technique was based on the open-flow IGRA method, and therefore is limited for use in estimating spatial variation in R_s, in contrast with static manual chambers that can be used for assessing spatial variation (e.g. Jia et al. 2003). Soil temperature and moisture directly affect respiration-related enzymatic activity. They also indirectly affect respiration via their effects on substrate supply (e.g.

phenology of plant C inputs, diffusion of substrates through soil air and water), and may vary with temporal and spatial scales. Because R_s depends on these multiple factors that are changing with global environmental changes, this type of analysis requires separating these processes in biogeochemical models to gain accurate predictions of future forest C sequestration. We encourage the use of AOCC combined with static manual chambers in support of efforts to obtain high-quality data on soil CO_2 efflux with high temporal and spatial resolution, because this type of data will be helpful for developing and validating process-based models.

CO_2 emissions from the 0–10 cm layer were sensitive to increases in soil moisture and contributed significantly to total soil CO_2 efflux. Therefore, soil moisture modulated the seasonal variation of soil CO_2 efflux at our site, a site that receives abundant precipitation with episodic rainfall during the Asia Monsoon. One of the most important findings in our study was that soil CO_2 efflux (g C m^{-2} $period^{-1}$) measured with AOCC during the snow-free season ranged from 979.8 $\pm$ 49.0 in 2005 to 1131.2 $\pm$ 56.6 in 2008, having coefficient of variation among years of only 6.4 % even with differences in soil moisture. This finding confirmed the results of a previous study by Mo et al. (2005b) which shows that inter-annual variability in R_s is small because litterfall input is fairly constant (Ohtsuka et al. 2009). However, at finer temporal scales, like daily and seasonal periods, soil CO_2 efflux was show to play a critical role in describing the variability of NEP, i.e. through enhanced daily soil CO_2 effluxes following episodic rainfall events, which can contribute to 32 % of the reduction in daily NEP associated with C source pulses to the atmosphere. Therefore, soil moisture is a secondary factor that determines NEP in the monsoon season together with solar radiation (Saigusa et al. 2005). Our results highlight the importance of precisely estimating responses of soil CO_2 efflux to changes in soil moisture following rainfall events when modeling seasonal C dynamics under climate change scenarios, even in humid monsoon regions.

Future studies are required to quantify the responses of autotrophic respiration from roots and heterotrophic respiration to soil moisture so that the related data can be used for predicting C sequestration in monsoon regions, and for designing strategies to mitigate the increasing atmospheric concentration of CO_2. These studies should be conducted in tandem with complementary process studies using long-term monitoring and coordinating with process models (Ito et al. 2014). Improving estimates of winter soil CO_2 efflux presents another challenge; combining new techniques such as vertical partitioning of CO_2 production within soil profile should prove useful (Yonemura et al. 2013), especially in a forest such as our site with snow cover from December to April. After many decades of research on the abiotic controls that are involved in the process of the decomposition of soil organic matter, we still lack robust process-based models and experiments that can be used to predict the consequences of changes in climate on the rates of decomposition within the global C budget (Moyano et al. 2013). One important aspect of process-based models that can be used to analyze the effects of soil moisture on R_s is the simulation of substrate accessibility (and thus of diffusion), which can be determined as a function of soil moisture, temperature and other interacting soil properties. For example, new experiments could address the question of how the plants may have a type of feedback on soil properties by changing soil quality through litterfall, substrate availability, or moisture content directly. Combining automated chamber techniques with monitoring the vertical profile of soil CO_2 production (Yonemura et al. 2013) could be a step forward in this direction. Fortunately, our AOCC system continues to measure soil CO_2 efflux during snow-free seasons, and we will report on the inter-annual variability of annual R_s, Q_{10} and R_{10} when more data become available.

Acknowledgments We thank Mr. K. Kurumado of the Institute for Basin Ecosystem Studies, Gifu University, and Mr. K. Abe of the National Institute for Agro-Environmental Sciences for their great support in the fieldwork. The 21st Century Centers of Excellence (COE) program "Satellite Ecology" at Gifu University supported this research. The Ministry of Agriculture, Forestry and Fisheries of Japan (Development of Mitigation Technologies to Climate Change in the Agricultural Sector, 2006–2010) also partly supported this work.

References

Bekku Y, Koizumi H, Oikawa T, Iwaki H (1997) Examination of four methods for measuring soil respiration. Appl Soil Ecol 5:247–254

Curiel Yuste J, Janssens IA, Ceulemans R (2005) Calibration and validation of an empirical approach to model soil CO_2 efflux in a deciduous forest. Biogeochem 73:209–230

Curiel Yuste J, Baldocchi DD, Gershenson A, Goldstein A, Misson L, Wong S (2007) Microbial soil respiration and its dependency on carbon inputs, soil temperature and moisture. Glob Change Biol 13:1–18

Davidson EA, Janssens IA (2006) Temperature sensitivity of soil carbon decomposition and feedbacks to climate change. Nature 440:165–173

Davidson EA, Belk E, Boone RD (1998) Soil water content and temperature as independent or confounded factors controlling soil respiration in a temperate mixed hardwood forest. Glob Change Biol 4:217–227

Davidson EA, Savage K, Bolstad P, Clark DA, Curtis PS, Ellsworth DS, Hanson PJ, Law BE, Luo Y, Pregitzer KS, Randolph JC, Zak D (2002) Belowground carbon allocation in forests estimated from litterfall and IRGA-based soil respiration measurements. Agri For Meteorol 113:39–51

Davidson EA, Janssens IA, Luo Y (2006a) On the variability of respiration in terrestrial ecosystems: moving beyond Q_{10}. Glob Change Biol 12:154–164

Davidson EA, Richardson AD, Savage KE, Hollinger DY (2006b) A distinct season pattern of the ratio of soil respiration to total ecosystem respiration in a spruce-dominated forest. Glob Change Biol 12:230–239

Fang J, Guo Z, Hu H, Kato T, Muraoka H, Son Y (2014) Forest biomass carbon sinks in East Asia, with special reference to the relative contributions of forest expansion and forest growth. Glob Chang Biol 20:2019–2030

Hashimoto T, Miura S, Ishizuka S (2009) Temperature controls temporal variation in soil CO_2 efflux in a secondary beech forest in Appi Highlands, Japan. J For Res 14:44–50

Hashimoto S, Morishita T, Sakata T, Ishizuka S (2011) Increasing trends of soil greenhouse gas fluxes in Japanese forests from 1980 to 2009. Sci Rep 1:116. doi:10.1038/srep00116

IPCC (2013) Climate Change 2013: The Physical Science Basis. http://www.buildingclimatesolutions.org/view/article/524b2c2f0cf264abcd86106a

Ito A, Saitoh TM, Sasai T (2014) Synergies between observational and modeling studies at the Takayama site: toward a better understanding of processes in terrestrial ecosystems. Ecol Res. doi:10.1007/s11284-2014-1205-7

Jia S, Akiyama T, Mo W, Inatomi M, Koizumi H (2003) Temporal and spatial variability of soil respiration in a cool-temperate broad-leaved forest. 1. Measurement of spatial variance and factor analysis. Jpn J Ecol 53:13–22 (in Japanese with English summary)

Joo SJ, Park SU, Park MS, Lee CS (2012) Estimation of soil respiration using automated chamber systems in an oak (*Quercus mongolica*) forest at the Nam-San site in Seoul, Korea. Sci Total Environ 416:400–409

Kim D-G, Mu S, Kang S, Lee D (2010) Factors controlling soil CO_2 effluxes and the effects of rewetting on effluxes in adjacent deciduous, coniferous, and mixed forests in Korea. Soil Biol Biochem 42:576–585

Kim D-G, Vargas R, Bond-Lamberty B, Turetsky MR (2012) Effects of soil rewetting and thawing on soil gas fluxes: a review of current literature and suggestions for further research. Biogeosci 9:2459–2483

Kirschbaum MUF (2010) The temperature dependence of organic matter decomposition: seasonal temperature variations turn a sharp short-term temperature response into a more moderate annually averaged response. Glob Chang Biol 16:2117–2129

Kuzyakov Y, Gavrichkova O (2010) Time lag between photosynthesis and carbon dioxide efflux from soil: a review of mechanisms and controls. Glob Chang Biol 16:3386–3406

Lee M-S, Nakane K, Nakatsubo T, Mo W, Koizumi H (2002) Effects of rainfall events on soil CO_2 efflux in a cool temperate deciduous broad-leaved forest. Ecol Res 17:401–409

Lee M-S, Nakane K, Nakatsubo T, Koizumi H (2005) The importance of root respiration in annual soil carbon fluxes in a cool-temperate deciduous forest. Agric For Meteorol 134:95–101

Lee M-S, Mo W, Koizumi H (2006) Soil respiration of forest ecosystems in Japan and global implications. Ecol Res 21:828–839

Lee M-S, Lee J-S, Koizumi H (2008) Temporal variation in CO_2 efflux from soil and snow surfaces in a Japanese ceder (*Crytomeria japonica*) plantation, central Japan. Ecol Res 23:777–785

Mo W, Nishimura N, Mariko S, Uchida M, Inatomi M, Koizumi H (2005a) Interannual variation in CO_2 effluxes from soil and snow surfaces in a cool-temperate deciduous broad-leaved forest. Phyton 45:99–107

Mo W, Lee MS, Uchida M, Inatomi M, Saigusa N, Mariko S, Koizumi H (2005b) Seasonal and annual variations in soil respiration in a cool-temperate deciduous broad-leaved forest in Japan. Agric For Meteorol 134:81–94

Moyano FE, Manzoni S, Chenu C (2013) Responses of soil heterotrophic respiration to moisture availability: an exploration of processes and models. Soil Biology Biochem 59:72–85

Muraoka H, Koizumi H (2005) Photosynthetic and structural characteristics of canopy and shrub trees in a cool-temperate deciduous broadleaved forest: implication to the ecosystem carbon gain. Agric For Meteorol 134:39–59

Ohtsuka T, Mo W, Satomura T, Inatomi M, Koizumi H (2007) Biometric based carbon flux measurements and net ecosystem production (NEP) in a temperate deciduous broad-leaved forest beneath a flux tower. Ecosystems 10:324–334

Ohtsuka T, Saigusa N, Koizumi H (2009) On linking multiyear biometric measurements of tree growth with eddy covariance-based net ecosystem production. Glob Chang Biol 15:1015–1024

Oishi AC, Palmroth S, Butnor JR, Johnsen KH, Oren R (2013) Spatial and temporal variability of soil CO2 efflux in three proximate temperate forest ecosystems. Agri For Meteorol 171–172:256–269

Pumpanen J, Kolari P, Ilvesniemi H, Minkkinen K, Vesala T, Niinistö S, Lohila A, Larmola T, Morero M, Pihlatie M, Janssens I, Yuste JC, Grünzweig JM, Reth S, Subke J-A, Savage K, Kutsch W, Østreng G, Ziegler W, Anthoni P, Lindroth A, Hari P (2004) Comparison of different chamber techniques for measuring soil CO_2 efflux. Agric For Meteorol 123:159–176

Saigusa N, Yamamoto S, Murayama S, Kondo H, Nishimura N (2002) Gross primary production and net ecosystem production of a cool temperate deciduous forest estimated by the eddy covariance method. Agric For Meteorol 112:203–215

Saigusa N, Yamamoto S, Murayama S, Kondo H (2005) Inter-annual variability of carbon budget components in and ASIAFLUX forest site estimated by long-term flux measurement. Agric For Meteorol 134:4–16

Satomura T, Hashimoto Y, Koizumi H, Nakane K, Nakatsubo T (2006) Seasonal patterns of fine root demography in a cool-temperate deciduous forest in central Japan. Ecol Res 21:741–753

Suh S-U, Chun Y-M, Chae N-Y, Kim J, Lim J-H, Yokozawa M, Lee M-S, Lee J-S (2006) A chamber system with automatic opening and closing for continuously measuring soil respiration based on an open-flow dynamic method. Ecol Res 21:405–414

Wang W, Chen W, Wang S (2010) Forest soil respiration and Its heterotrophic and autotrophic components: global patterns and responses to temperature and precipitation. Soil Biol Biochem 42:1236–1244

Yonemura S, Yokozawa M, Shirato Y, Nishimura S, Nouchi I (2009) Soil CO_2 concentrations and their implications in conventional and no-tillage agricultural fields. J Agric Meteorol 65:141–149

Yonemura S, Yokozawa M, Sakurai G, Kishimoto-Mo AW, Lee N, Murayama S, Ishijima K, Shirato Y, Koizumi H (2013) Vertical soil-air CO_2 dynamics at the Takayama deciduous broadleaved forest AsiaFlux site. J For Res 18:49–59